Supplementary Material for

Morphological Regulation on Barium Titanate Perovskite Particles for Broadening Microwave Absorption in GHz and THz Range

Yu-Kai Luo[1†], Hai-Sen Gao[1†], Yichuan Zhang[1*], Kai Zhang[3], Xiao-Juan Lei[4], Ming Wang[1,2*]

[1]Academy for Advanced Interdisciplinary Studies, School of Chemistry and Chemical Engineering, Southwest University, Chongqing, 400715, P. R. China.

[2]State Key Laboratory of Solid Lubrication, Lanzhou Institute of Chemical Physics, Chinese Academy of Sciences, Lanzhou, 730000, P. R. China.

[3]School of Materials and Energy, Southwest University, Chongqing, 400715, P. R. China.

[4]College of Food Science, Southwest University, Chongqing, 400715, P. R. China.

[†]The authors are equal to this work. *Address correspondence to Yichuan Zhang, zhangyichuan@swu.edu.cn and Ming Wang, mwang@swu.edu.cn

Table S1 Lattice parameters of BTO samples.

Sample	**a=b=c(Å)**	**V_0(Å^3)**
BTO-0	4.00503	64.24
BTO-1	4.01934	64.93
BTO-2	4.02353	65.14
BTO-3	4.02898	65.40
BTO-0_{14}	4.01894	64.91
BTO-1_{14}	4.02158	65.04
BTO-2_{14}	4.02644	65.28
BTO-0_{180}	4.00267	64.13
BTO-1_{180}	4.00961	64.46
BTO-2_{180}	4.00988	64.48

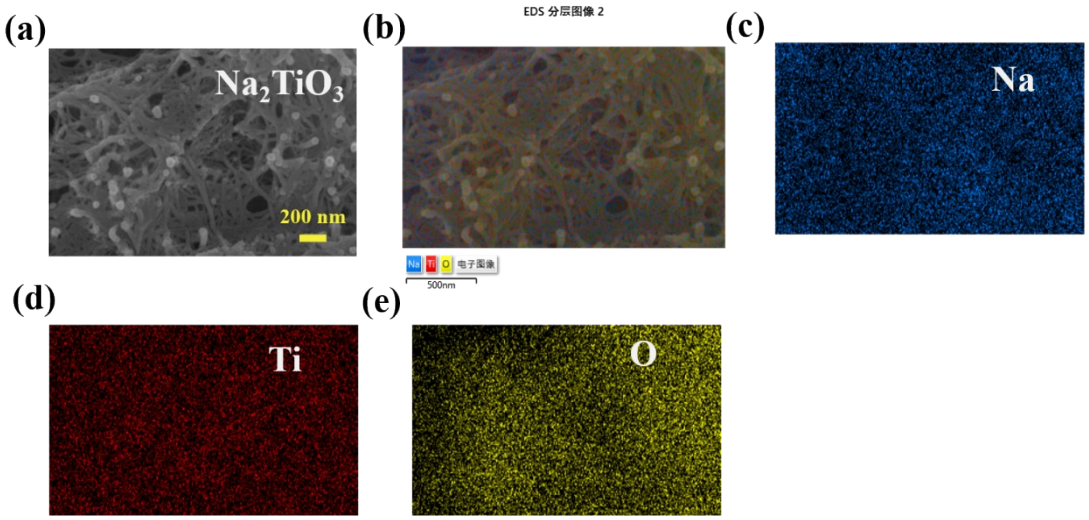

Fig. S1. (a) SEM image for the NTO sample, (b) is the EDS image of NTO, (c-e) are the EDS images of Na, Ti, and O for NTO, respectively.

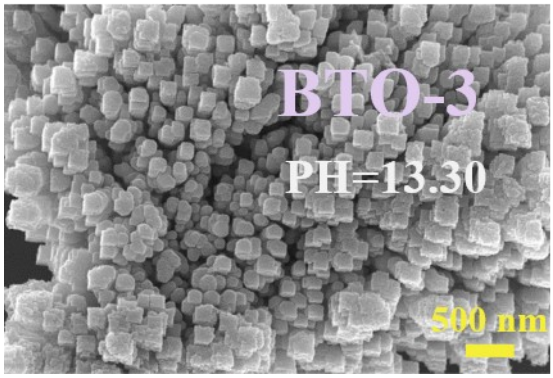

Fig. S2. SEM image for BTO-3.

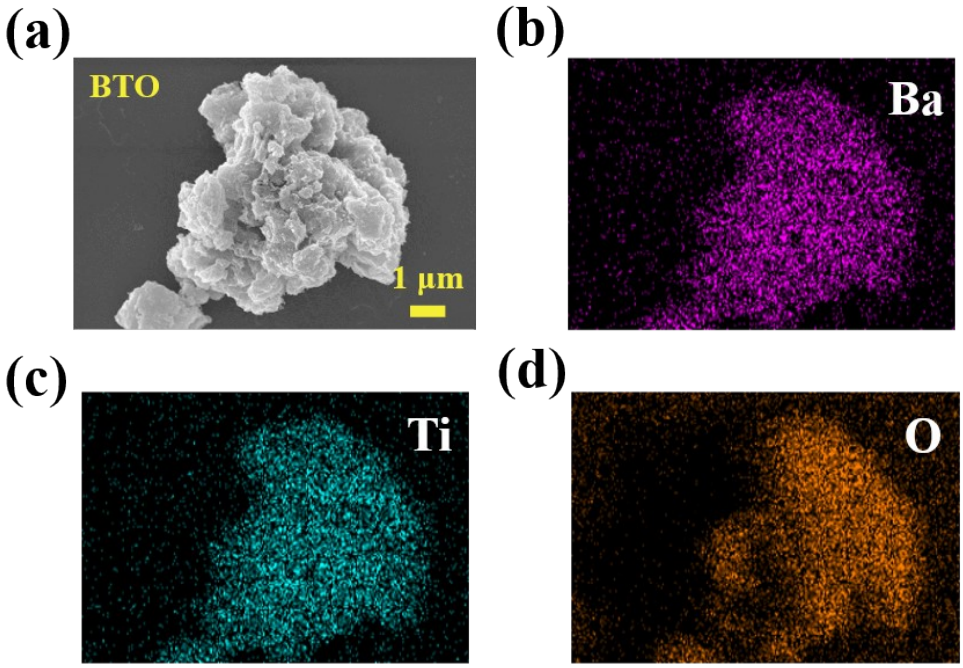

Fig. S3. The EDS element mappings of BTO perovskites based on SEM.

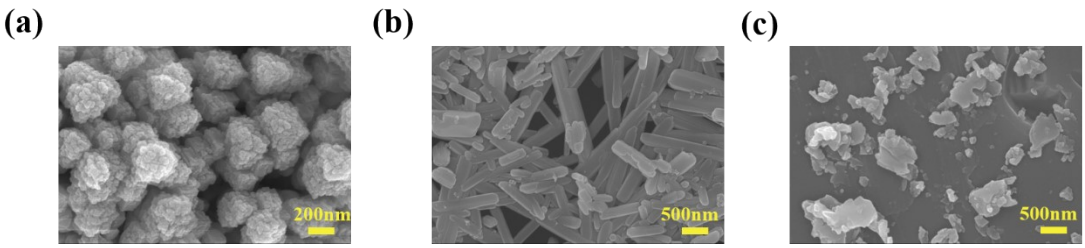

Fig. S4. SEM images for the BTO samples. (a) BTO-3, (b) BTO-1, and (c) BTO-2.

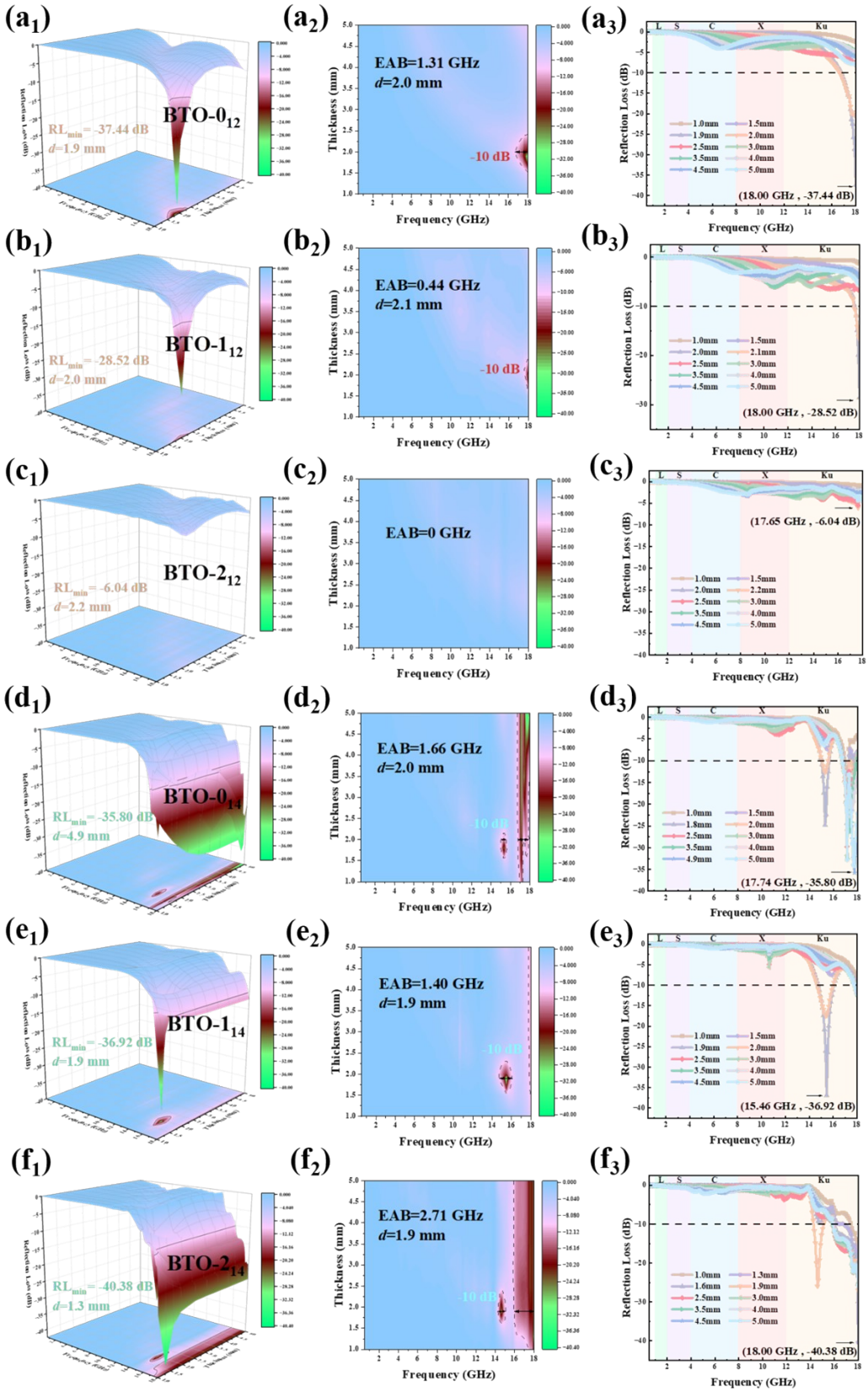

Fig. S5. Frequency dependence of 3D RL, 2D RL mapping, and 1D RL curve of (a_1-a_3) the BTO-0_{12}, (b_1-b_3) BTO-1_{12}, (c_1-c_3) BTO-2_{12}, (d_1-d_3) BTO-0_{14}, (e_1-e_3) BTO-1_{14}, and (f_1-f_3) BTO-2_{14}, respectively.

Fig. S5 presents the MA performance of BTO samples synthesized under different hydrothermal pH conditions. As shown in Fig. S5(a_1-a_3), BTO-0_{12} achieves an RL_{min} of -37.44 dB at 18.00 GHz with a thickness of 1.9 mm. The EAB is 1.31 GHz (16.69–18.00 GHz) with a matching thickness of 2.0 mm. Fig. S5(b_1-b_3) shows that BTO-1_{12} achieves an RL_{min} of -28.52 dB at 18.00 GHz with a thickness of 2.0 mm. The EAB is 0.44 GHz (17.56–18.00 GHz) with a matching thickness of 2.1 mm. As shown in Fig. S5(c_1-c_3), BTO-2_{12} achieves an RL_{min} of -6.04 dB at 17.65 GHz with a thickness of 2.2 mm. The EAB is 0 GHz, indicating poor absorption performance. Fig. S5(d_1-d_3) shows that BTO-0_{14} achieves an RL_{min} of -35.80 dB at 17.74 GHz with a thickness of 4.9 mm. The EAB is 1.66 GHz (15.02–15.55 GHz and 16.78–17.91 GHz) with a matching thickness of 2.0 mm. As shown in Fig. S5(e_1-e_3), BTO-1_{14} achieves an RL_{min} of -36.92 dB at 15.46 GHz with a thickness of 1.9 mm. The EAB is 1.66 GHz (15.02–15.55 GHz and 16.78–17.91 GHz) with a matching thickness of 2.0 mm. Fig. S5(f_1-f_3) shows that BTO-2_{14} achieves an RL_{min} of -40.38 dB at 18.00 GHz with a thickness of only 1.3 mm. The EAB is 2.71 GHz (14.33–15.03 GHz and 15.99–18.00 GHz) with a matching thickness of 1.9 mm.

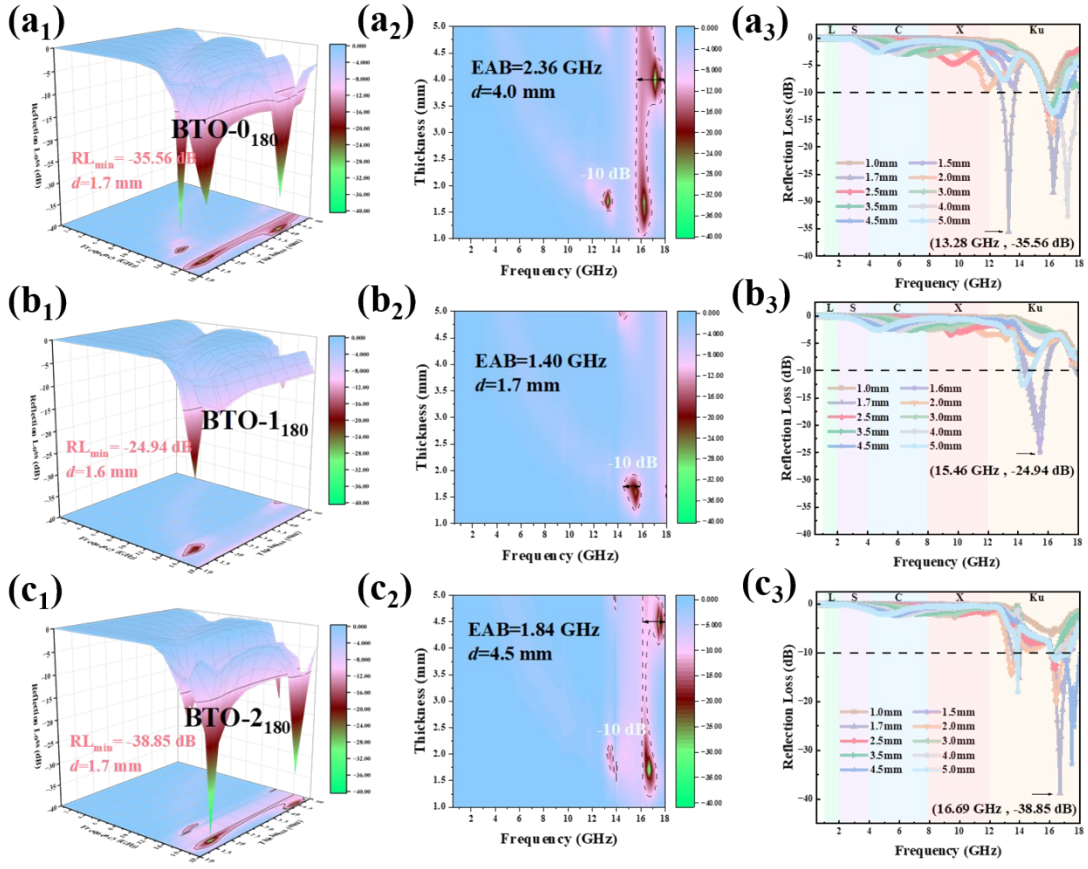

Fig. S6. Frequency dependence of 3D RL, 2D RL mapping, and 1D RL curve of (a_1-a_3) the BTO-0_{180}, (b_1-b_3) BTO-1_{180}, and (c_1-c_3) BTO-2_{180}, respectively.

Fig. S6 presents the MA performance of BTO samples synthesized under different hydrothermal temperatures. As shown in Fig. S6(a_1-a_3), BTO-0_{180} achieves an RL_{min} of -35.56 dB at 13.28 GHz with a thickness of 1.7 mm. The EAB is 2.36 GHz (15.64–18.00 GHz) with a matching thickness of 4.0 mm. Fig. S6(b_1-b_3) shows that BTO-1_{180} achieves an RL_{min} of -24.94 dB at 15.46 GHz with a thickness of 1.6 mm. The EAB is 1.40 GHz (14.41–15.81 GHz) with a matching thickness of 1.7 mm. As shown in Fig. S6(c_1-c_3), BTO-2_{180} achieves an RL_{min} of -38.85 dB at 16.69 GHz with a thickness of 1.7 mm. The EAB is 1.84 GHz (14.41-15.81GHz) with a matching thickness of 4.5 mm.

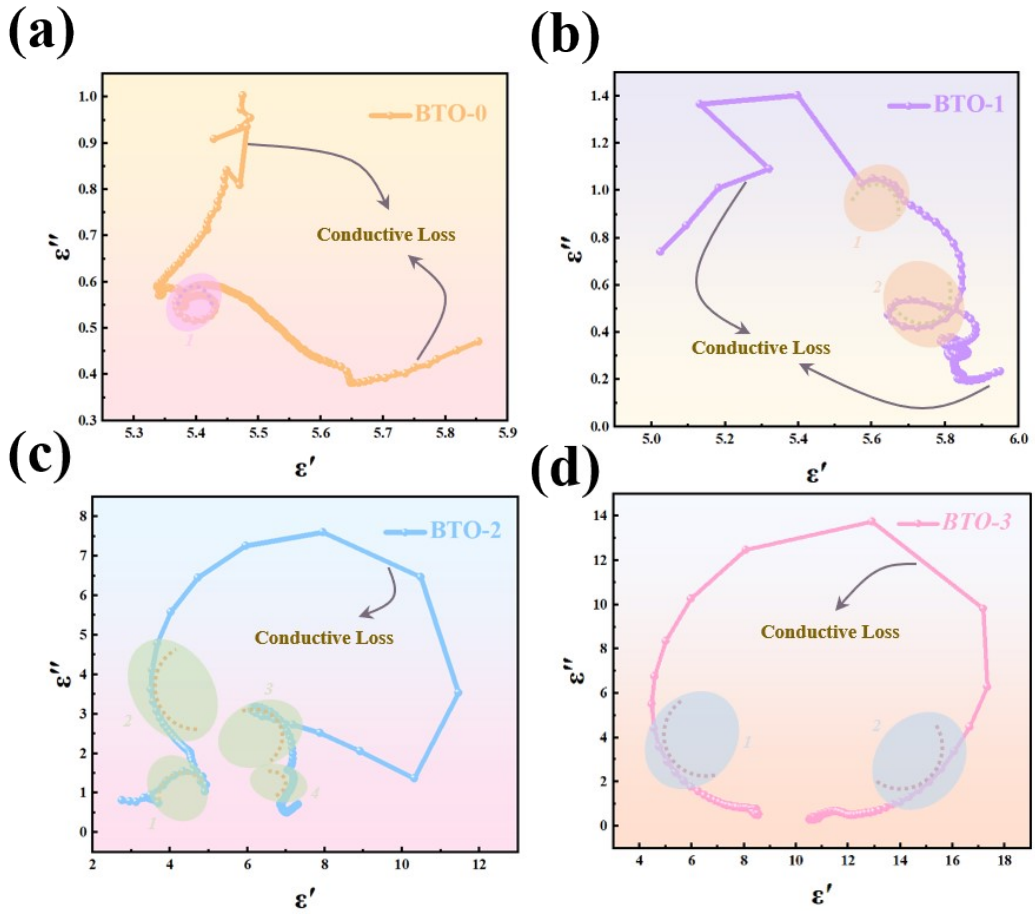

Fig. S7. Cole–Cole curves of the BTO samples. (a) BTO-0, (b) BTO-1, (c) BTO-2, and (d) BTO-3.